Internal Arc CFD Simulation of Long Single Phase HV-GIS

Ostrowski J., Galletti B., Hencken K., Lehmann J., Seeger M.

All authors are with ABB Corporate Research, Segelhofstrasse 1k, CH-5405 Baden, Switzerland, e-mail: joerg.ostrowski@ch.abb.com

A novel one-dimensional CFD-tool for the simulation of the pressure build up during internal arc faults in long single phase High Voltage SF6 Gas Insulated Switchgear (HV-GIS) is presented in this paper. We do not use the common empirical thermal transfer coefficient (Kp factor) in our tool. Instead a more physically motivated approach has been developed and is introduced here. The approach includes important cooling mechanisms that prevent excess gas/plasma-temperatures and subsequent numerical instabilities. In order to understand if the approach is valid, we prescribe the arc-energy from a benchmark experiment. Then we compare the simulated pressure build-up curve with the measured pressure build-up.

Keywords: internal arc, simulation, CFD, high voltage, gas insulated switchgear, SF6-Al

1 INTRODUCTION

Fault arcs in SF6 insulated HV-GIS are rare but very dangerous events that cannot fully be avoided. The electrical energy that is released by the arc heats up the gas and leads to a high overpressure. Cracks in the metal enclosure of the GIS can be generated, or the enclosure could even explode. Parts may fly away into the installation room and harm personnel. Bursting disks are therefore integrated into the enclosure that limit the overpressure and avoid an uncontrolled explosion. However hot SF6 gas that is a big threat to our atmosphere is released also in case the bursting disks opens in a controlled way, for example during an internal arc test. The goal of internal arc simulations [1, 2] is therefore to predict the transient pressure build up in order to correctly design the bursting disk and to reduce the number of experimental tests. Commonly used are 0D-simulation tools [1, 3] that do not compute a 3D spatial distribution of the flow quantities like pressure P or temperature T, but that compute a kind of average value of each quantity in the entire gas volume.

2 SIMULATION MODEL

A picture of a long single phase SF6 insulated HV-GIS is shown in Fig. 1 at the end of this article. It consists of a long inner conductor and an enclosure that are both to a large extent cylindrically symmetric, and that are made of aluminum. The aspect ratio between the length and the diameter of the HV-GIS is high, larger than 10. After arc ignition cold gas is compressed at either end of the HV-GIS and hinders the outflow of the gas at the bursting disk which is usually located there. In order to factor in this effect, we cannot apply the standard 0D-simulation approach. Instead we have to account for the spatial distribution of the flow quantities along the principal axial direction. Therefore we implemented a one-dimensional compressible CFD solver. Flow variations in the radial direction were neglected, but we accounted for variations of the flow cross section. A full 3D CFD simulation of such a complex and long geometry would be difficult to mesh and would also be very time consuming (simulation time at least a week on computer clusters of the current generation). Thus such a simulation would not be feasible in a product design unit. Our 1D approach in contrast enables to use only a few parameters to describe the geometry, see Fig.2. Meshing is automatized and simulation times are about 6 hours. Thus such a 1D simulation can also be carried out in a product design unit. We do not resolve the arc itself in our simulation, because this would require a fine mesh of the thin arc in order to simulate in a stable fashion the balances between the electrical heating and the radiation losses, or between the pressure gradient and the electro-magnetic Lorentz force. Instead we inject the electrical energy in a volume that is larger than the arc itself. Thus all gradients are lower than in reality and the simulation is stable. In this paper we call this volume the arc-volume. In the standard model the energy-input is usually scaled by the thermal transfer coefficient Kp that represents the amount of electrical energy that is used to heat up the gas. Such an approach is intrinsically unstable. The instability can easily be understood:

The electrical energy-input leads to a pressure increase in the arc-volume compared to the environment, thus mass is ejected from the arc-volume, the density drops, and the temperature explodes if further energy is injected. In reality there are cooling mechanisms that limit this temperature rise. These are radiation and electrode evaporation. Thus we included these cooling mechanisms into our model.

A sketch of the most important effects is given in Fig. 3. The arc attaches at the inner conductor and at the enclosure that are both made of aluminum. The aluminum evaporates at the arc roots during arcing [4]. The evaporation temperature is approximately 3500 K, significantly lower than the arc-temperature. That's the reason why electrode evaporation is a cooling mechanism. The evaporated aluminum mixes with the SF6 gas and the important exothermal reaction between SF6 and aluminum [5] has to be included in the energy balance. This is accomplished by simulation of the movement of the evaporated aluminum in the SF6 gas and minimizing the free Gibbs energy with respect to the resulting spatial concentration under the assumption of local thermal equilibrium [6]. Radiation transport is another cooling mechanism that we solve by using a 1D-Discrete Ordinates Method (DOM) into the principal direction. We neglected the energy loss by heat conduction through the enclosure, thus we used adiabatic boundary conditions for the CFD solver. We also neglected the electro-magnetic Lorentz-forces for simplicity. However we did include arc-movement into the simulation: We averaged the gas velocity in a volume (diameter 30 cm) around the arc and moved it with this average velocity. After the opening of the bursting-disk the arc moved into the direction of the bursting-disk, because there is a strong flow in this direction. When the arc reached a spacer we artificially reduced the arc-velocity about a factor of 5 in order to mimic the pervasion of the arc through the spacer. To summarize, we modelled the process by using the following ingredients:

- Compressible 1D-CFD
- Radiation transport
- Electrode evaporation
- Aluminum species transport
- P,T, concentration dependent material data
- Arc-movement

3 RESULTS

In order to check if the approach is valid we simulated the case that is depicted in Fig. 1. An internal arc test has been carried out with this device and the transient pressure build-up at the two ends of the GIS has been measured. The volume of the GIS was 0.38 m^3 and the rated short-circuit current of 50Hz/65kA (RMS) released an electrical power of 28 MW during 342 ms of arcing. The initial filling pressure of the SF6 gas was 5.3 Bar, and the bursting disk that was located at the left end of the GIS with an outflow area of 86 cm^2 opened at an absolute pressure of 12.2 Bar after 102 ms. The absolute peak pressures were 21.6 Bar and 24.5 Bar and were reached after approximately 270 ms.

In the simulation we discretized the 5.5 m long GIS with 2'750 elements in the axial direction. The time-step size was chosen as 50 ns. The simulation was stable (also with alternative geometries, e.g. without spacers). It took 6 hours for 0.5 s. We used a discharge coefficient of 0.8 for the bursting disk. This value was extracted from a stationary 3D CFD simulation of the bursting disk and the exhaust that has been carried out beforehand. The arc was ignited at a distance of 2.1 m from the left end, next to a spacer at 2 m with 120 cm^2 opening. It took some time for the arc to pervade the spacer.

The simulation nicely reproduced the measured pressure build-up at both ends. The burst disk opened after 90 ms, and the overshooting of the pressure was also fairly well reproduced. Note that the simulated pressure started to drop before the arc-extinction. Only the time to reach the peak pressures was slightly delayed about approximately 80 ms. Fig. 5 gives an impression of the spatial distribution of the temperature and the density after 300 ms. Note that the temperature is realistic and not extensively high even at the arc position at 2 m where the arc stays at the spacer in this moment. As mentioned the cold dense gas is compressed at both ends of the GIS and blocks the outflow through the burst disk that is located at the left end of the GIS at 0.3 m.

4 CONCLUSIONS

We implemented a stable 1D-CFD tool for simulation of internal arcs in long single phase SF6 insulated HV-GIS. Stability is achieved by taking into account cooling mechanisms. The usage of a thermal transfer coefficient Kp was avoided. A first benchmark showed convenient agreement between simulation and measurement. Further benchmarks are necessary to confirm the validity of this approach.

REFERENCES

[1] Cigre Working group A3.24, Tools for the simulation of effects of the internal arc in transmission and distribution switchgear, 2014.

[2] Kahlen J C, Pietsch G, Reduzierung der Druckbeanspruchung elektrischer Anlagen im Störlichtbogenfall, Schlussbericht AiF, 2011.

[3] Dullni E, Wojcik P, Bleszynski T, Feeling the pressure: Simulating pressure rise in switchgear installation rooms, ABB Review Simulation, 3/2013.

[4] Zhang X, Modellierung der Auswirkungen von Störlichtbögen in elektrischen Anlagen, Dissertation, RWTH Aachen, 2002.

[5] Schumann H, Untersuchungen zum Druckanstieg in Schotträumen SF6-isolierter, einpolig metallgekapselter Hochspannungs-Schaltanlagen infolge stromstarker Lichtbögen, Dissertation, Darmstadt, 1989.

[6] Doiron C, Hencken K, Calculation of thermodynamic and transport properties of thermal plasmas based on the Cantera software toolkit, In: Proceedings of the XXII Europhysics Conference on Atomic and Molecular Physics of Ionized Gases, Greifswald, July 15-19, 2014.

Fig.1: Picture of a long single phase HV-GIS. It is 5.5m long and has a diameter of 30 cm

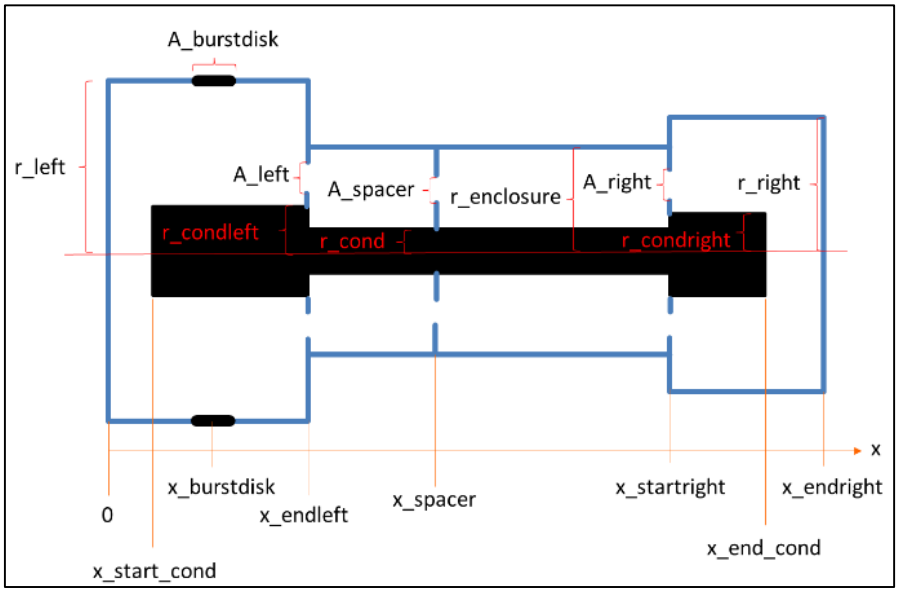

Fig.2: Parameters for the geometrical definition of a 1D-simulation of a long single-phase HV-GIS

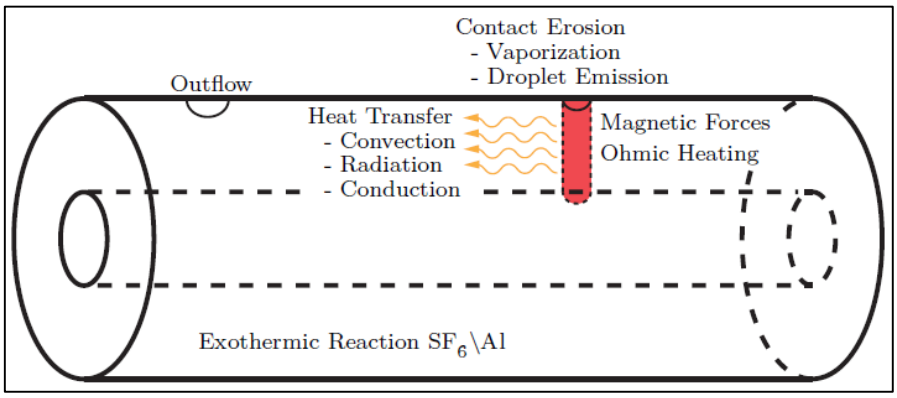

Fig.3: Sketch of the effects during an internal arc fault

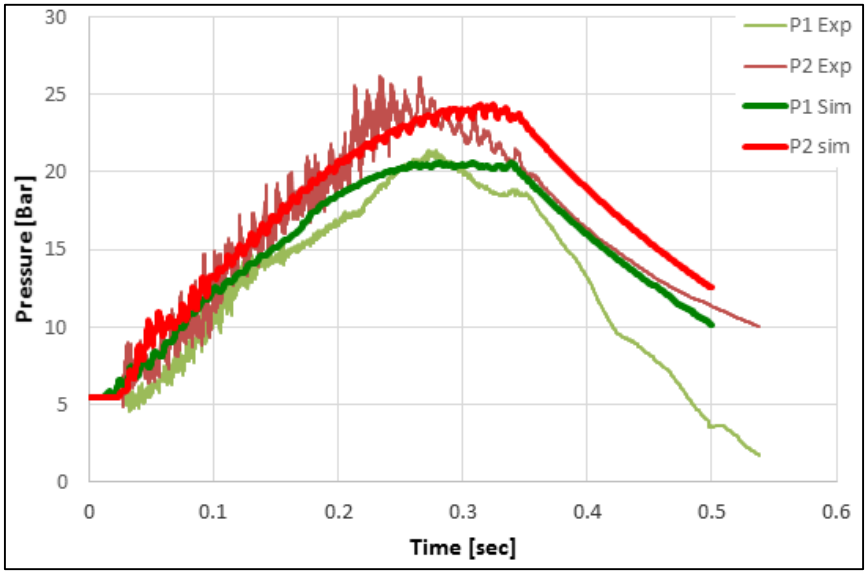

Fig.4. Pressure build-up at the two ends of the long HV-GIS. Comparison Experiment vs Simulation

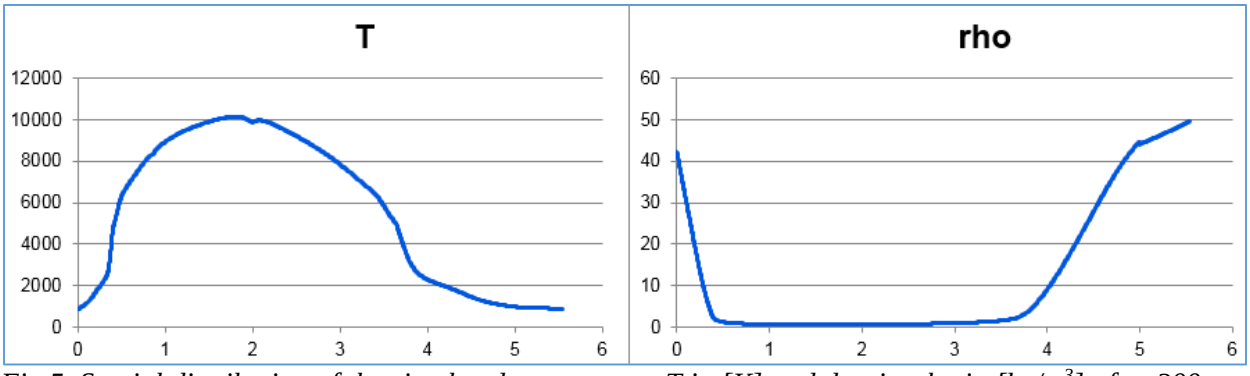

Fig.5. Spatial distribution of the simulated temperature T in [K] and density rho in [kg/m^3] after 300 ms along the principal direction [m] of the 5.5 m long GIS